Revista Facultad de Ingeniería
Journal Homepage: https://revistas.uptc.edu.co/index.php/ingenieria

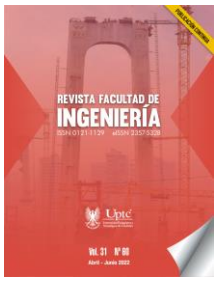

Theoretical and Practical Determination of a Binary Mixture of AISI 316 Steel Powders to Increase Corrosion Resistance in Powder Metallurgical Parts

Luz-Adriana Cañas-Mendoza[1]
Yaneth Pineda-Triana[2]
Enrique Vera-Lopez[3]

Received: June 05, 2022 **Accepted:** August 25, 2022 **Published:** September 06, 2022

Citation:
L.-A. Cañas-Mendoza, Y. Pineda-Triana, E. Vera-Lopez, "Determination of a Binary Mixture of AISI 316 Steel Powders to Increase Corrosion Resistance in Powder Metallurgical Parts," *Revista Facultad de Ingeniería*, vol. 31 (61), e14417, 2022. https://doi.org/10.19053/01211129.v31.n61.2022.14417

[1] Ph. D. (c) Universidad Tecnológica de Pereira (Pererira-Risaralda, Colombia). luzadriana@utp.edu.co. ORCID: 0000-0001-6872-6068
[2] Ph. D.Universidad Pedagógica y Tecnológica de Colombia (Tunja-Boyacá, Colombia). yaneth.pineda@uptc.edu.co. ORCID: 0000-0002-5561-9412
[3] Ph. D. Universidad Pedagógica y Tecnológica de Colombia (Tunja-Boyacá, Colombia). enrique.vera@uptc.edu.co. ORCID: 0000-0003-4150-9308

Abstract

Powder metallurgical steels have lower corrosion resistance compared to wrought steels. Their behavior is simultaneously affected by interconnected porosity, pore morphology, interaction with sintering atmospheres, and metallurgical phenomena such as steel 'sensitization'. This work presents the theoretical methodology to calculate the optimum composition of the mixture and the conditions for a maximum packing of two sizes spheres (assuming a spherical shape factor) according to the development published by Brouwers for a system of binary mixtures. For the theoretical determination of the mixture, the results of density and porosity of a 316 powder metallurgical stainless steel made from prealloyed powders of two average granulometries (45µm and 150µm) are presented. The powders were combined in different proportions to define the appropriate quantities that allow the manufacture of steel with a low corrosion rate. The obtained results confirm that the theoretical calculation is a reliable alternative to formulate powder metallurgical alloys since good particle packing is achieved, which has a favorable effect on the characteristics of the finished product.

Keywords: austenitic stainless steels; corrosion rate; powder metallurgy; sintered density; sintered porosity.

Determinación teórica y práctica de una mezcla binaria de polvos de acero AISI 316 para aumentar la resistencia a la corrosión en piezas pulvimetalúrgicas

Resumen

Los aceros pulvimetalúrgicos tienen una menor resistencia a la corrosión en comparación con los aceros forjados. Su comportamiento se ve afectado simultáneamente por la porosidad interconectada, la morfología de los poros, la interacción con las atmósferas de sinterización y fenómenos metalúrgicos como la "sensitización" del acero. Este trabajo presenta la metodología teórica para calcular la composición óptima de una mezcla y las condiciones requeridas para obtener un empaquetamiento máximo de esferas de dos tamaños promedio de partículas (asumiendo un factor de forma esférico) según la investigación publicada por

Brouwers para un sistema de mezclas binarias. Para la determinación teórica de la mezcla se presentan los resultados de densidad y porosidad de un acero inoxidable pulvimetalúrgico 316 elaborado a partir de polvos prealeados de dos granulometrías promedio (45µm y 150µm). Los polvos se combinaron en diferentes proporciones, con el fin de definir las cantidades adecuadas que permitan fabricar un acero con bajos valores de su velocidad de corrosión. Los resultados obtenidos confirman que el cálculo teórico es una alternativa confiable para formular aleaciones pulvimetalúrgicas, ya que se logra un alto empaquetamiento de partículas, lo cual incide favorablemente en las características del producto terminado.

Palabras clave: aceros inoxidables austeníticos; densidad de sinterizado; porosidad de sinterizado; pulvimetalurgia; velocidad de corrosión.

Determinação teórica e prática de uma mistura binária de pós de aço AISI 316 para aumentar a resistência à corrosão em peças metalúrgicas do pó

Resumo

Os aços metalúrgicos em pó apresentam menor resistência à corrosão em comparação aos aços forjados. Seu comportamento é afetado simultaneamente pela porosidade interligada, morfologia dos poros, interação com atmosferas de sinterização e fenômenos metalúrgicos como a "sensibilização" do aço. Este trabalho apresenta a metodologia teórica para calcular a composição ótima de uma mistura e as condições necessárias para obter um empacotamento máximo de esferas de dois tamanhos médios de partículas (assumindo um fator de forma esférica) de acordo com a pesquisa publicada por Brouwers para um sistema de misturas. binário. Para a determinação teórica da mistura, são apresentados os resultados de densidade e porosidade de um aço inoxidável metalúrgico de pó 316 feito a partir de pós pré-ligados de duas granulometrias médias (45µm e 150µm). Os pós foram combinados em diferentes proporções, a fim de definir as quantidades adequadas que permitam a fabricação de um aço com baixos valores de sua taxa de corrosão. Os resultados obtidos confirmam que o cálculo teórico é uma alternativa confiável para formular ligas metalúrgicas do pó, uma vez que se

consegue um alto empacotamento de partículas, o que afeta favoravelmente as características do produto acabado.

Palavras-chave: aços inoxidáveis austeníticos; densidade sinterizada; metalurgia do pó; porosidade sinterizada; taxa de corrosão.

I. INTRODUCTION

Powder Metallurgy (PM) as a manufacturing process is the production of parts from metal powders. The conventional route can be summarized in the stages of mixing, compaction, sintering, and, some cases, finishing activities. Compaction is intended to achieve the shape, density, and contact between particles, so the finished part reaches enough resistance and can continue its processing; this is called a preform or green compact. The distribution of particle sizes is a key factor for the final properties of the product due to the porosity that remains during compaction [1]. This can be reduced by introducing smaller particles that, when located in the void spaces, contribute to obtaining higher density values [2]. Sintering as the consolidation stage leads the green compact formed by individual particles to a coherent body under high temperature in a controlled atmosphere. The nature and strength of the bonds between particles depend on the mechanisms of diffusion, plastic flow, evaporation of volatile substances in the compressed, recrystallization, grain growth, and pore contraction [3]. Shape and other characteristics of the powders are controlled to produce preforms with apparent density ranging between 2.5 and 3.2 g/cm^3, enough green resistance, and good compressibility; the highest green densities are typically obtained for austenitic steels [4]. The corrosion resistance of sintered steels has been improved by reducing their porosity by increasing compaction pressure and sintering temperature, or through infiltration processes. Improvements are also achieved with the addition of alloying and the selection of a proper sintering atmosphere. In works such as Moral's *et al.* [5], a reduction in the porosity of a PM ferritic stainless steel was observed through the addition of small spherical powders atomized in gas to the traditional irregular and larger powders (atomized in water) in samples processed by the conventional metal powder route. Improvements in resistance against corrosion were revealed by potentiodynamic polarization tests.

It is important to keep in mind that due to the thermal cycles typical of the powder metallurgy process, austenitic stainless steels tend to precipitate carbides of $M_{23}C_6$ forms in an approximate range of temperatures between 450°C and 950°C, even from few time intervals. Carbides tend to deposit at grain boundaries, generating a

concentration gradient of the predominant metallic element in its composition; as M can be replaced by Cr, Fe or Mo carbides of the form $(Cr,Fe,Mo)_{23}C_6$ or $(Cr_{16}Fe_5Mo_2)C_6$ will be generated [6]. The above generates a decrease in the carbide-forming species M, which primarily tends to be chromium. Additionally, the concentration of this element around the precipitated carbides reaches values lower than the required 10% for the passivation of steel. The effect of this phenomenon is known as sensitization, and it causes located intergranular corrosion. This paper presents the results obtained by analyzing alloys made with AISI 316 stainless steel powders of two average particle sizes (45µm and 150µm) to reduce the porosity level. The manufacturing route was conventional powder metallurgy. The theoretical definition of the optimal composition was calculated with the development published by Browers [1], which is based on the previous work of Furnas [7] for binary mixtures, following the procedure below:

- Calculation of u ratio from the diameters d_L y d_S of the largest and smallest particles, respectively, from the equation (1).

$$u = \left(\frac{d_L}{d_S}\right) = \frac{150\ \mu m}{45\ \mu m} = 3.33 \qquad (1)$$

- Selection of this u value (3.33) in Table1 presented by Browers to extract the proposed data, where C_L and C_S correspond to the volumetric fraction of the largest and smallest constituents, respectively. From these values, the relation $r = \frac{C_L}{C_S}$ is observed. h represents the void fraction between particles as a function of the u ratio and the volumetric fraction C_L, calculated by Furnas [7].

- Conversion of the fractions for each size using the density value of AISI 316 steel (7.96 g/cm^3), obtaining that the percentage of each particle fraction in an optimal mix is: 64% wt.-% of 150 µm powders, plus 36% wt.-% of 45 µm powders.

Table 1. Mixing conditions for maximum bimodal packing of spheres [1].

$u = \left(\frac{d_L}{d_S}\right)$	$C_L = k(u)$	$C_S = 1 - C_L$	$r = g(u)$	$h[u, r = g(u)]$
1	0.5	0.5	1	0.5
2	0.52	0.48	1.083	0.474
2.5	0.54	0.46	1.174	0.440
3.33	**0.64**	**0.36**	**1.778**	**0.412**
5	0.66	0.34	1.941	0.376
10	→2/3	→1/3	→2	0.328

DOI: https://doi.org/10.19053/01211129.v31.n61.2022.14417

$u = \left(\frac{d_L}{d_S}\right)$	$C_L = k(u)$	$C_S = 1 - C_L$	$r = g(u)$	$h[u, r = g(u)]$
20	→2/3	→1/3	→2	0.314
50	→2/3	→1/3	→2	0.270

II. METHODOLOGY

A. Raw Materials Characterization

The powders' chemical composition was consolidated from technical data sheets provided by the producer GOODFELLOW[1], and the composition was verified through Energy Dispersion Spectrometry (EDS), Atomic Absorption (AA), and X-Ray Diffraction (DRX). The morphology was determined by means of Scan Electron Microscopy (SEM), as well as the shape factor, measuring the length and width of 30 particles for each sample of the acquired images. The aspect ratio (AR) was calculated with equation (2).

$$AR = {}^{d_{max}}/_{d_{min}} \qquad (2)$$

B. Sample Preparation and Characterization

Five mixes called metallic matrixes were defined, with the compositions in Table 2. Metallic powders and zinc stearate ($Zn(C_{18}H_{35}O_2)_2$) used as a lubricant (1% wt.-%) were mixed in a planetary mill without solid grinders for 20 minutes at 150 rpm.

Table 2. Powder combinations for the preparation of metallic matrixes to be evaluated.

Metallic powder	Matrix 1 (wt.-%)	Matrix 2 (wt.-%)	Matrix 3 (wt.-%)	Matrix 4 (wt.-%)	Matrix 5 (wt.-%)
AISI 316 (150 µm)	100	50	**65**	20	0
AISI 316 (45 µm)	0	50	**35**	80	100

The uniaxial compaction was performed at a pressure of 800 MPa in a universal Microtest EM/500/FR machine; pressure was defined from previous work by Perez [8]. Preforms with a diameter of 10 mm (±0,15) and height of 4 mm (±0,1) were obtained. Morphology, microstructure, and porosity were observed through sweep electron microscopy (SEM). Porosity was defined by the analysis of 30 images for each sample; density was measured based on the ASTM B962 standard [9].

Matrixes were sintered in a tubular furnace CARBOLITE STF/TZF in a grade four nitrogen atmosphere, with a dew point of -60°C [10,11]. The sintering temperature was defined from recommended values for powder metallurgical austenitic stainless steels and was set at 1200ºC [10-19]. Heating was carried out from room temperature to 450°C with a 20-minute hold to remove the lubricant, and then up to sintering temperature (1200°C) with a 30-minute hold, at a rate of 5°C/min; finally, samples were removed for cooling in air to room temperature.

C. Corrosion Rate of Sintered Samples

A GAMRY-750 potentiostat/galvanostat was used to measure the linear polarization resistance (LPR) and obtain the Tafel curves. With the equation proposed by Butler-Volmer around low polarization values (±20mV with respect to E_{corr}), the linear response between current and voltage was confirmed by determining the slopes ba and bc. The corrosion rate was calculated through converting the current density to its equivalent in mils/year (mpy). The ASTM G5-94 [20] standard guidelines were followed using a 1N H_2SO_4 electrolyte with 250ppm NaCl, reference electrode (Ag/AgCl 3M KCl), and platinum counter-electrode.

III. Results and Discussion

Table 3 shows the chemical composition, and Figures 1 and 2 show the diffractograms obtained by DRX and the morphology of the metal powders.

Table 3. Chemical composition of AISI 316 powders.

Element (wt.-%)	AISI/SAE 316 (45µm)			AISI/SAE 316 (150µm)		
	Producer	EDS	AA	Producer	EDS	AA
Cr	16.5 – 20.0	18.11	19.9	16.5 – 20.0	17.06	19.8
Ni	8.0 – 14.0	9.9	9.73	8.0 – 14.0	10.45	9.486
Mo	2.5 – 3.5	2.17	---	2.5 – 3.5	2.18	---
Mn	<2	---	0.118	<2	---	0.104
C	<0.08	---	---	<0.08	---	---
Si	---	0.96	0.645	---	1.23	0.605
Ti	---	0.03	0.015	---	0.022	0.014
Fe	Balance	Balance	66.3	Balance	Balance	66.33

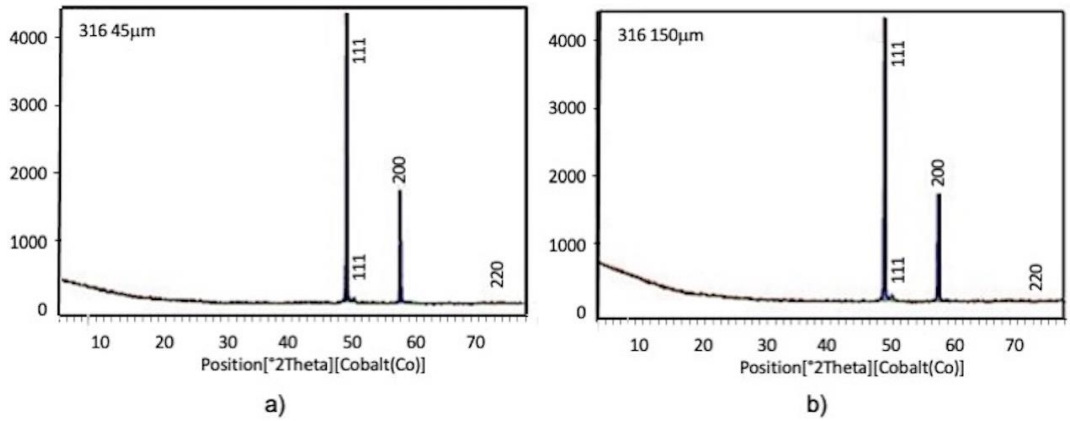

Fig. 1. AISI 316 steel powder diffractogram a) 45µm; b) 150µm.

The results confirm that the composition ranges are typical of austenitic stainless steel. For both types of samples, diffraction patterns (111), (200) and (220) are observed corresponding to the face-centered cubic structure of austenite. This confirms the specified by the manufacturer. The average Aspect Ratio (AR) for the 45 µm powders was 1.4406 and for the 150 µm powders was 1.5692, showing that the particles have an irregular shape typical of powders obtained by atomization with water (Figure 2). Moreover, the observed morphology is appropriate for favouring the compaction and sintering processes for the alloys.

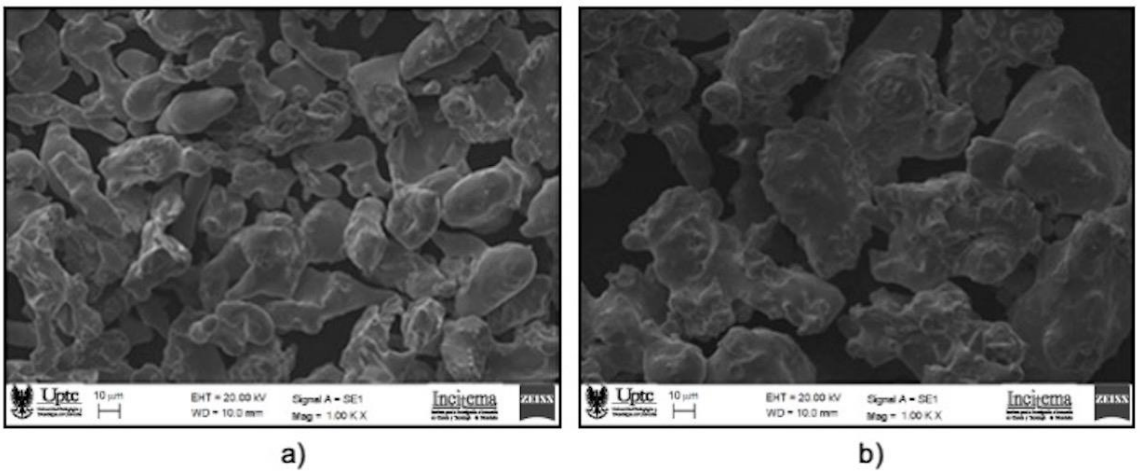

Fig. 2. AISI 316 steel powder morphology at 1000X a) 45µm; b) 150µm.

Table 4 compiles the results of the variables determined by the electrochemical method. The high corrosion rates were attributed to the aggressiveness of the electrolyte in terms of pH and the presence of chloride ions (Cl^-).

Table 4. Results of the potentiodynamic polarization tests.

Sample	ba [mV/decade]	bc [mV/decade]	i_{corr} [mA/cm^2]	E_{corr} [mV]	LPR [Ohms]	Vcorr [mpy]
Matrix 1	56.81	81.47	0.0799	-487	233	36.0
Matrix 2	84.47	89.40	0.0583	-500	415	26.3
Matrix 3	35.16	33.89	0.0237	-500	406	10.7
Matrix 4	32.42	33.45	0.0396	-495	232	17.8
Matrix 5	78.30	109.60	0.0529	-489	480	23.9

The graphs in Figure 3 show the typical behaviour of stainless steel with an anodic zone that represents the passivation potential (i_p), due to the formation of the Cr_2O_3 species, and a transpassivation zone by the breaking of the passive layer at high polarizations.

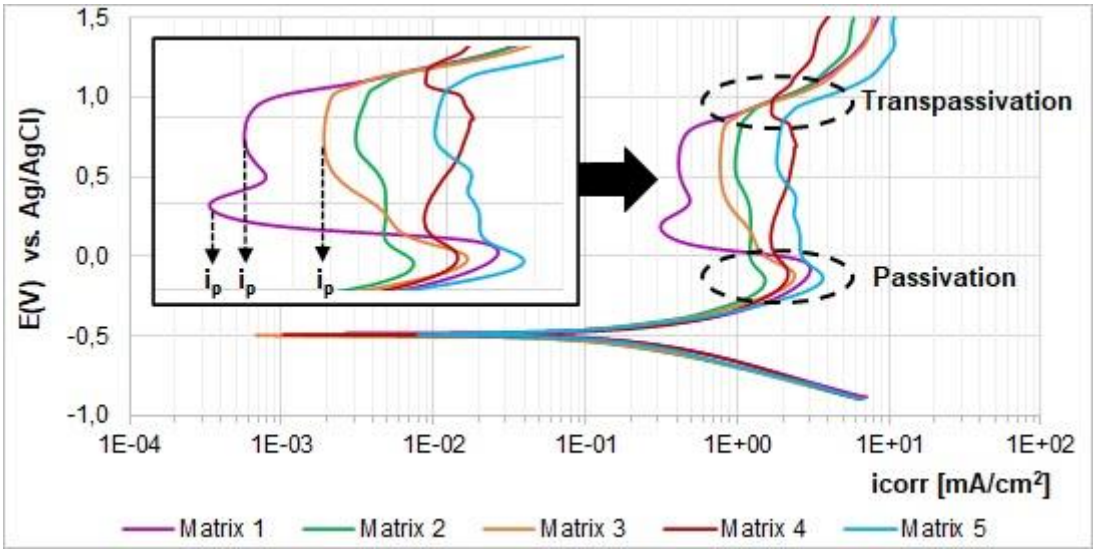

Fig. 3. Tafel curves of potentiodynamic polarization of the evaluated matrixes.

In the internal box of Figure 3, passivation is observed. It is evident that this film presents an unstable behaviour (before reaching the transpassivation potential), and in Matrix 1, which presented the highest values of corrosion rates, the greatest

instability of the passive layer compared to the other samples was shown. For the rest of the samples, the decrease in the anodic current towards the passivation current (i_p) is less pronounced, even though their corrosion rate values are lower compared to Matrix 1. Matrix 3, the one that presented the lowest corrosion rate, shows the progressive formation of the passive film, and it tends to be relatively stable once formed before reaching the transpassivation potential. The other samples present weak transpassivation (high values of i_p) and unstable films due to their breaking and regeneration, which is evidenced by the variation of the current in the passive region.

The consolidated results in Figure 4 include the porosity values of the preforms and sintered samples on the abscissas, on the left axis, the density of the sintered alloys, and on the right axis, the corrosion rate. The consolidated results in Figure 4 were positioned in order of increasing porosity, showing that Matrix 3 has the lowest porosity. The results in Figure 4 were sorted in order of increasing porosity, showing that Matrix 3 has the lowest porosity and the highest density, favouring the results of the corrosion rate. On the contrary, Matrix 1, composed of large particles of a single size, presented the opposite behaviour. The change in density and porosity of the preforms compared to the sintered is related to the “coalescence of particles” typical of sintering.

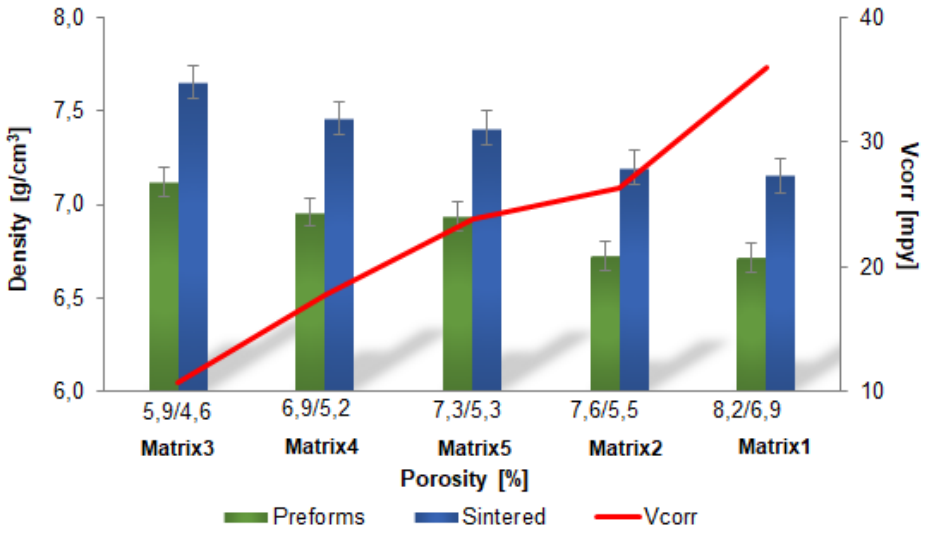

Fig. 4. Relationship between density, porosity, and corrosion rate.

Based on the chemical composition, the “Thermo-Calc” software was used to predict phases from the sintering temperature, which confirms the theoretical presence of austenite with 96% and the possibility of carbides precipitation $Cr_{23}C_6$ with a proportion of 4%. As presented in the introduction above, this species is the cause of sensitization of austenitic stainless steel [10-11,15,18] (Figure 5).

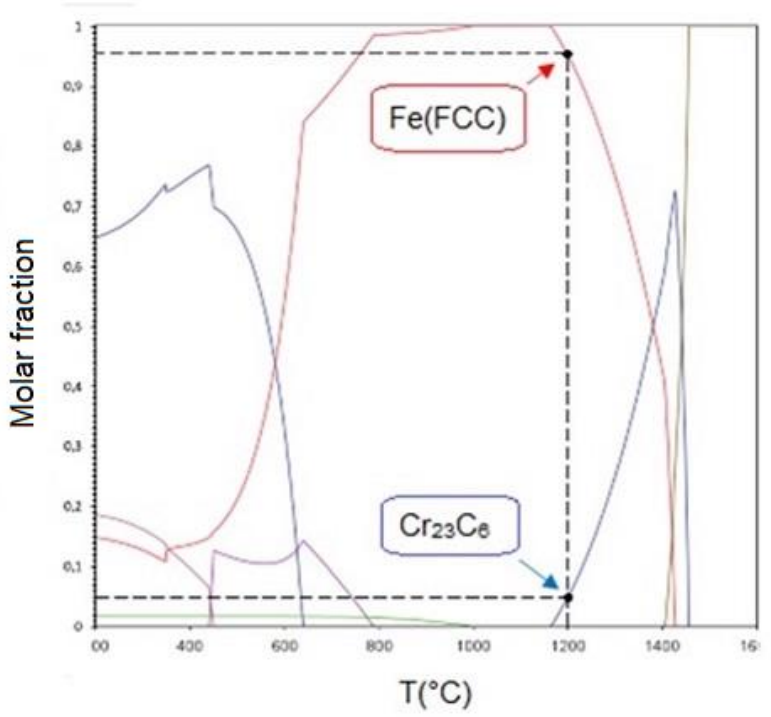

Fig. 5. Molar fraction of phases vs. temperature (Thermo-Calc).

Through elemental mapping with SEM-EDRX (Energy Dispersive X-Ray Spectroscopy), Figure 6 was obtained with backscattered electrons, showing the presence of austenite (g) along with unconnected open porosities of rounded and elongated morphology. Carbides of the $Cr_{23}C_6$ form preferentially precipitate at the grain boundaries on the surface of the pores, with small deposits inside the grains. There is a coincidence with the projected structure with “Thermo-Calc”, although the observed percentage of carbides exceeds that predicted by the software because of the low cooling rate after sintering which favours the precipitation.

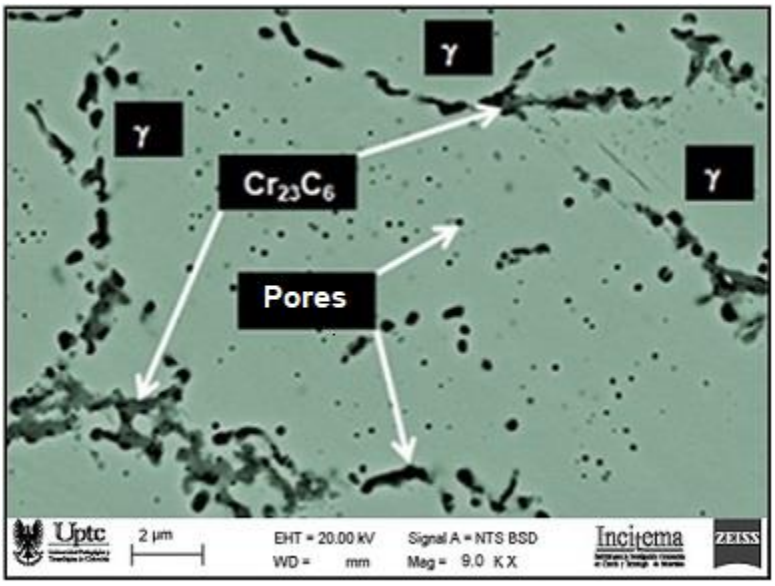

Fig. 6. Microstructure observed for Matrix 3, obtained by MEB-EDRX.

From the microstructural observation, it is found that despite the higher density values for the called Matrix 3 (65% of 150 mm powders; 35% of 45 mm powders), the remaining porosity is quite critical and generates favourable conditions for the sensitization of steel. The elongated porosities are possible locations of crack nucleation, which requires further analysis of the mechanical properties of the alloy. In terms of corrosion resistance, the importance of controlling cooling rates from sintering temperatures in such a way as to inhibit the precipitation of chromium carbides is demonstrated. Therefore, the synthesis of the samples with rapid cooling (in water) after the sintering of the samples is suggested since the current thermal cycles applied favour intergranular corrosion phenomena due to the effect of sensitization.

IV. Conclusions

An inverse relationship between porosity degree and sample density obtained by powder metallurgy was observed, and the effect of these properties on corrosion rate. The obtained results coincide with theoretical approaches for combinations of particle sizes, defining an optimum binary mix of AISI 316 powders of 65 wt.-% (150 µm) / 35 wt.-% (45 µm), which showed the lowest corrosion rate.

The sintering stage is of key importance in processing powder metallurgy pieces from stainless steel and involves several factors that generate synergistic effects on the quality of the final pieces. Among these primary factors to consider are the thermal cycles since, depending on material chemical composition, it is possible to have phase precipitation such as $Cr_{23}C_6$ chromium carbides, which in the case of austenitic stainless steels generates the sensitization that further induces intergranular corrosion. The results of the current work allow us to conclude that a rapid cooling stage after sintering is necessary to avoid the formation of those carbides.

The conventional powder metallurgy process applied to austenitic stainless steels demands strict control of the operating variables as the response to the corrosion of these materials depends on the synergist effects of factors such as: chemical composition (which directly affects the quality of the passive layer and therefore the efficiency of the protection against the surrounding environment), the presence of precipitates, composes or intermetallic phases (which act unfavourably on corrosion resistance) and the interconnected porosity that increases the exposed surface area.

AUTHORS' CONTRIBUTION

Luz-Adriana Cañas-Mendoza: Investigation; Validation; Formal Analysis; Writing – original draft.

Yaneth Pineda-Triana: Investigation; Validation; Formal Analysis; Writing – review & editing.

Enrique Vera-Lopez: Investigation; Validation; Formal Analysis; Writing – review & editing.

REFERENCES

[1] H. J. H. Brouwers, "Particle-size distribution and packing fraction of geometric random packings," *Physical Review E - Statistical, Nonlinear, and Soft Matter Physics*, vol. 74, no. 3, e031309, 2006. https://doi.org/10.1103/PhysRevE.74.031309

[2] S. Schmid, S. Kalpakjian, *Manufactura, Ingeniería y Tecnología*. Quinta Edición, México, 2008, p. 491

[3] M. Groover, *Fundamentos de manufactura moderna: Materiales, procesos y sistemas*, 3rd ed. McGraw-Hill, 2007, p.499.

[4] P. W. Lee The Timken Co et al., *ASM Handbook Vol. 7. Powder Metal Technologies and Applications*, 1998, p. 309.

[5] C. Moral, A. Bautista, F. Velasco, "Aqueous corrosion behaviour of sintered stainless steels manufactured from mixes of gas atomized and water atomized powders," *Corrosion Science*, vol. 51, no. 8, pp. 1651–1657, 2009. https://doi.org/10.1016/j.corsci.2009.04.017

[6] C. C. Furnas, Department of Commerce, Bureau of Mines, *Report of Investigation Serial No. 2894, 1928*; Bulletin of US Bureau of Mines 307, 74 , 1929

[7] S. P. Pérez Velázquez, *Evaluación de la resistencia al desgaste y a la corrosión de un MMC sinterizado por plasma*, Universidad Pedagógica y Tecnológica de Colombia, Tunja, 2015

[8] ASTM B962-15, *Standard Test Methods for Density of Compacted or Sintered Powder Metallurgy (PM) Products Using Archimedes' Principle*, 2015

[9] G. S. Upadhyaya, *Powder metallurgy technology*, 1st ed. Cambridge: Cambridge International Science Publishing, 2002, p. 91

[10] C. García, F. Martin, Y. Blanco, "Effect of sintering cooling rate on corrosion resistance of powder metallurgy austenitic, ferritic and duplex stainless steels sintered in nitrogen," *Corrosion Science*, vol. 61, pp. 45–52, 2012. https://doi.org/10.1016/j.corsci.2012.04.021

[11] A. Pardo, M. C. Merino, A. E. Coy, F. Viejo, R. Arrabal, E. Matykina, "Pitting corrosion behaviour of austenitic stainless steels - combining effects of Mn and Mo additions," *Corrosion Science*, vol. 50, no. 6, pp. 1796–1806, 2008. https://doi.org/10.1016/j.corsci.2008.04.005

[12] E. Zengin, H. Ahlatci, H. Zengin, "Investigation of microstructure, tribological and corrosion properties of AISI 316L stainless steel matrix composites reinforced by carbon nanotubes," *Materials Today Communication*, vol. 29, e102758, 2021. https://doi.org/10.1016/j.mtcomm.2021.102758

[13] T. Takeda, K. Tamura, H. Trans. Brucher, "Pressing and Sintering of Chrome-Nickel Austenitic Stainless Steel Powders," *Journal of the Japan Society of Powder and Powder Metallurgy*, vol. 17, no. 2, pp. 70–76, 1970

[14] C. García, F. Martin, Y. Blanco, "Effect of sintering cooling rate on corrosion resistance of powder metallurgy austenitic, ferritic and duplex stainless steels sintered in nitrogen," *Corrosion Science*, vol. 61, pp. 45–52, 2012. https://doi.org/10.1016/j.corsci.2012.04.021

[15] F. Velasco, J. M. Ruiz-Román, J. M. Torralba, J. M. Ruiz-Prieto, "Corrosion resistance of alloyed powder metallurgy austenitic stainless steels in acid solutions," *British Corrosion Journal*, vol. 31, no. 4, pp. 295-299, 1996. https://doi.org/10.1179/bcj.1996.31.4.295

[16] L. Fedrizzi, A. Molinari, F. Deflorian, A. Tiziani, P. L. Bonora, "Corrosion study of industrially sintered copper alloyed 316L austenitic stainless steel", *British Corrosion Journal*, vol. 26, pp. 46–50, 1991

[17] M. Rosso, "Contribution to study and development of PM stainless steels with improved properties," *Journal of Achievements in Materials and Manufacturing Engineering*, vol. 24, no. 1, pp. 178–187, 2007

[18] G. S. Upadhyaya, *Powder metallurgy technology*, 1st ed. Cambridge: Cambridge International Science Publishing, 2002

[19] ASTM G5-94 *Standard Reference Test Method for Making Potentiostatic and Potentiodynamic Anodic Polarization Measurements,* 2004